TEXT4SEG: REIMAGINING IMAGE SEGMENTATION AS TEXT GENERATION

Anonymous authors
Paper under double-blind review

ABSTRACT

Multimodal Large Language Models (MLLMs) have shown exceptional capabilities in vision-language tasks; however, effectively integrating image segmentation into these models remains a significant challenge. In this paper, we introduce Text4Seg, a novel *text-as-mask* paradigm that casts image segmentation as a text generation problem, eliminating the need for additional decoders and significantly simplifying the segmentation process. Our key innovation is *semantic descriptors*, a new textual representation of segmentation masks where each image patch is mapped to its corresponding text label. This unified representation allows seamless integration into the auto-regressive training pipeline of MLLMs for easier optimization. We demonstrate that representing an image with 16×16 semantic descriptors yields competitive segmentation performance. To enhance efficiency, we introduce the Row-wise Run-Length Encoding (R-RLE), which compresses redundant text sequences, reducing the length of semantic descriptors by 74% and accelerating inference by $3\times$, without compromising performance. Extensive experiments across various vision tasks, such as referring expression segmentation and comprehension, show that Text4Seg achieves state-of-the-art performance on multiple datasets by fine-tuning different MLLM backbones. Our approach provides an efficient, scalable solution for vision-centric tasks within the MLLM framework.

1 INTRODUCTION

Multimodal Large Language Models (MLLMs) (Yin et al., 2023) have successfully extended the capabilities of powerful Large Language Models (LLMs) into the visual domain. Recent advancements demonstrate the remarkable ability of these models to engage in natural language-based human-computer interaction and text-based reasoning over visual inputs (Liu et al., 2024c; Lu et al., 2024; Liu et al., 2024a; Bai et al., 2023; Chen et al., 2024). MLLMs have emerged as powerful tools for vision-centric tasks, including image generation (Song et al., 2024; Wang et al., 2024c), object detection (Wang et al., 2024a; Ma et al., 2024; Zhang et al., 2023) and semantic segmentation (Lai et al., 2024; Zhang et al., 2024b). However, seamlessly integrating MLLMs with these tasks, particularly in dense prediction tasks like semantic segmentation, remains challenging due to the intrinsic differences between language and visual modalities.

A straightforward approach adopted by most existing works (Lai et al., 2024; Xia et al., 2024; Zhang et al., 2024b; He et al., 2024; Ren et al., 2024; Rasheed et al., 2024; Zhang et al., 2023; Wu et al., 2024) involves appending additional visual decoders (*e.g.*, SAM (Kirillov et al., 2023)) to MLLMs, as illustrated in Fig. 1(a). While effective, this combination presents several limitations: 1) it complicates the end-to-end training pipeline with additional loss functions; 2) it requires careful modifications to MLLM architectures, leading to unexpected challenges when scaling up the training. VisionLLM (Wang et al., 2024a) attempts to convert segmentation masks into polygon coordinate sequences, as shown in Fig. 1(b). However, the performance is often unsatisfactory, as LLMs may struggle to associate polygon coordinates with shapes, leading to the reintroduction of segmentation-specific decoders in VisionLLMv2 (Jiannan et al., 2024). Finding a more effective method to unlock the segmentation capabilities for MLLMs remains crucial. Such method should adhere to the next-token prediction paradigm of MLLMs for easier optimization, require fewer architectural changes for better scalability, and fully leverage text generation capabilities of LLMs.

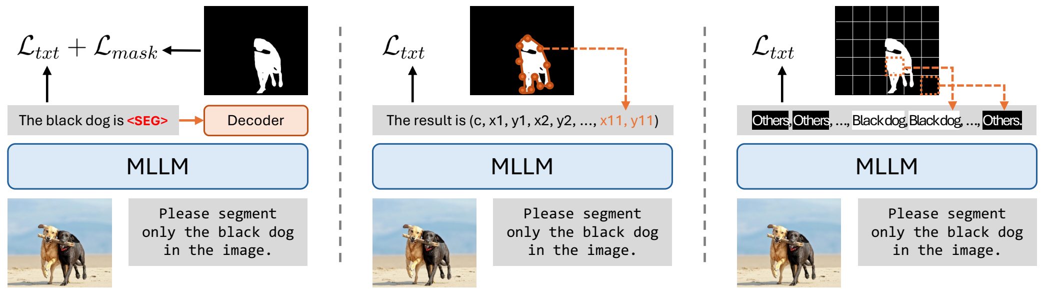

(a) *embeddings-as-mask* (b) *polygon coordinates* (c) *text-as-mask*

Figure 1: Different paradigms of MLLMs based image segmentation: (a) *embeddings-as-mask* paradigm that relies on additional segmentation decoder and loss (*e.g.*, LISA (Lai et al., 2024)); (b) *polygon coordinates* for instance segmentation (*e.g.*, VisionLLM (Wang et al., 2024a)); (c) our *text-as-mask* paradigm that relies on semantically consistent text sequences.

In this paper, we introduce a novel *text-as-mask* paradigm that casts image segmentation as a text generation problem, which significantly simplifies the segmentation process. We propose **Text4Seg**, a decoder-free framework for MLLMs based image segmentation, as illustrated in Fig. 1(c). Central to our method is a novel sequence representation of segmentation masks. Instead of using index masks or numerical coordinates, we map each flattened patch of the input image to its corresponding text description (*e.g.*, a semantic label, a short phrase, or a long sentence), forming a purely textual representation of images, named as **semantic descriptors**. This representation offers several advantages: 1) a unified sequence representation seamlessly integrated into the auto-regressive training pipeline, making joint optimization with text tasks easier; 2) no architectural changes are required, allowing full utilization of existing MLLM training infrastructure, making it ideal for scaling up; 3) support for large label vocabularies, equivalent to semantic words; and 4) flexible switching between referring expression segmentation, open-vocabulary segmentation, and other visual grounding tasks.

Inspired by ViT (Dosovitskiy et al., 2021), we demonstrate that *representing an image with 16 $\times$ 16 semantic words, i.e.,* 256 *length of semantic descriptors, is sufficient to achieve satisfactory results*. To improve efficiency, we introduce the Row-wise Run-Length Encoding (R-RLE), which compresses the repeated descriptors within each image row while preserving the spatial structure. *Without compromising performance*, R-RLE achieves a 74% reduction in semantic descriptors length and speeds up inference by $3\times$ on average. To further enhance performance, we apply an off-the-shelf mask refiner, *i.e.*, SAM, as a post-processing method to obtain pixel-level segmentation masks.

With the proposed semantic descriptors, training MLLMs for segmentation requires minimal additional effort. We begin by constructing instruction-following data from existing segmentation datasets, transforming the vanilla semantic masks into the semantic descriptors format, and then fine-tuning the model using query-response conversations. This approach applies to a variety of vision-centric tasks, such as referring expression segmentation, open-vocabulary segmentation, and visual grounding tasks. Our experiments demonstrate that Text4Seg can seamlessly integrate segmentation capabilities into existing MLLM architectures, such as LLaVA-1.5 (Li et al., 2024a), Qwen-VL (Bai et al., 2023), DeepseekVL (Lu et al., 2024), and InternVL2 (Chen et al., 2023b), *without any architectural modifications*. Without bells and whistles, Text4Seg consistently achieves superior or comparable performance to previous models, highlighting its efficiency, flexibility, and robustness. In summary, our key contributions are as follows:

- We propose Text4Seg, a novel *text-as-mask* paradigm that redefines image segmentation as a text generation problem, fully leveraging the text generation capabilities of MLLMs.
- We introduce semantic descriptors, a textual sequence representation of segmentation masks that seamlessly integrates with existing MLLMs for easier optimization. We demonstrate that 16×16 semantic descriptors are sufficient for achieving strong performance.
- We develop Row-wise Run-Length Encoding (R-RLE) to compress semantic descriptors, significantly reducing its length and inference costs without compromising performance.
- We validate the effectiveness and robustness of Text4Seg based on various MLLMs backbones by achieving state-of-the-art performance across various vision centric tasks.

2 Related Work

Multimodal Large Language Models. MLLMs are typically developed by enhancing large language models (LLMs) with visual perception modules, which can generate coherent textual conversations grounded in multimodal inputs. For instance, Flamingo (Alayrac et al., 2022) introduces the Perceiver Resampler, which connects a pre-trained vision encoder with LLMs for effective few-shot learning. OpenFlamingo (Awadalla et al., 2023) and Otter (Li et al., 2023a) build upon this architecture with a focus on multi-modal in-context instruction tuning. BLIP-2 (Li et al., 2023b) and InstructBLIP (Dai et al., 2023) bridge the modality gap using a lightweight Querying Transformer (Q-Former), demonstrating enhanced performance on zero-shot vision-to-language tasks. The LLaVA seires (Liu et al., 2024c;a) employs a linear layer or MLP as a modality connector, trained on multimodal language-image instruction-following data generated with GPT-4, showcasing notable capabilities in multimodal chat interactions. They demonstrate impressive capabilities in multimodal chat interactions. In contrast, Qwen-VL (Bai et al., 2023) and mPLUG-Owl2 (Ye et al., 2024) explore feature compression to a fixed length through cross-attention mechanisms with learnable queries, optimizing computational efficiency. Recent advancements (Liu et al., 2024b; Xu et al., 2024; Li et al., 2024a;b;c; Lin et al., 2023) have focused on enhancing visual encoding through high-resolution inputs. For example, LLaVA-UHD (Xu et al., 2024) implements an image modularization strategy, segmenting native-resolution images into smaller, variable-sized slices to improve scalability and encoding efficiency. Similarly, LLaVA-NEXT (Liu et al., 2024b) and LLaVA-OneVision (Li et al., 2024a) utilize the AnyRes scheme to accommodate high-resolution image inputs. In this work, we present Text4Seg to endow existing MLLMs with image segmentation capabilities based on instruction tuning, *without necessitating any changes to their architecture*.

Language-Guided Semantic Segmentation and Localization. Recent advancements have enabled MLLMs to incorporate task-specific modules for vision-centric tasks. LISA (Lai et al., 2024) introduces the embedding-as-mask paradigm, utilizing a special `<seg>` token to prompt a segmentation mask decoder, such as SAM (Kirillov et al., 2023), thereby enhancing performance in reasoning and referring expression segmentation. Building on this, GSVA (Xia et al., 2024) employs multiple `<seg>` tokens and a `<REJ>` token to address cases where users reference multiple subjects or provide descriptions mismatched with image targets. Similarly, GLaMM (Rasheed et al., 2024) extends LISA's single-object focus by integrating natural language responses with corresponding object segmentation masks. They introduce a large-scale, densely annotated Grounding-anything Dataset to train GLaMM, which significantly improves performance across various vision tasks. OMG-LLaVA (Zhang et al., 2024a) and PixelLM (Ren et al., 2024) are also capable of grounded conversation generation. PixelLM (Ren et al., 2024) advances LISA further by replacing SAM with a lightweight pixel decoder and introducing a comprehensive segmentation codebook for efficient multi-target reasoning and segmentation. In contrast, GROUNDHOG (Zhang et al., 2024b) proposes inputting visual entity tokens, rather than visual tokens, using their masked feature extractor, which enables fine-grained visual understanding. GROUNDHOG also curated a grounded visual instruction tuning dataset with Multi-Modal Multi-Grained Grounding, M3G2, to fully train the model. Recent studies (Zhang et al., 2023; Jiannan et al., 2024; Wu et al., 2024; Fei et al., 2024) extend MLLMs to vision-centric tasks like visual grounding (*e.g.*, bounding boxes, masks) by integrating task-specific heads for different applications. While effective, these approaches increase training complexity and limit model scalability due to multiple decoders and loss functions. Other efforts (Chen et al., 2021; Peng et al., 2023; Wang et al., 2024a) have sought to simplify this process by learning coordinate sequences or location tokens. However, they tend to perform well only in object detection tasks with simple location coordinates, and struggle to achieve competitive results on more complex tasks such as segmentation. In contrast, we introduce a general sequence representation for vision tasks without task-specific heads, enabling seamless integration with MLLMs and leveraging their text-generation capabilities for effective, versatile performance across applications.

3 Methodology

In this section, we begin with an overview of MLLMs in Sec. 3.1. Next, we elaborate on the design of semantic descriptors and row-wise run-length encoding in Sec. 3.2. Finally, we show how to construct visual instruction data to train our proposed Text4Seg in Sec. 3.3.

3.1 PRELIMINARY

Multimodal Large Language Models (MLLMs) (Yin et al., 2023) refer to the LLM-based models with the ability to process, reason, and generate response from multimodal information. Typically, as shown in Fig. 2, an MLLM can be abstracted into three main components: 1) a pre-trained vision encoder, which is responsible for extracting visual tokens from input images, 2) a pre-trained large language model (LLM), which handles reasoning and generating outputs, and 3) a modality connector, which acts as a bridge between the vision encoder and the LLM.

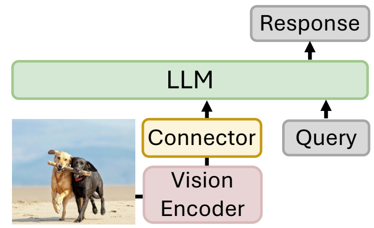

Figure 2: MLLM architecture.

3.2 SEMANTIC DESCRIPTORS

Definition of semantic descriptors. Our semantic descriptors are inspired by ViT (Dosovitskiy et al., 2021), which represents an image as 16×16 visual tokens. As illustrated in Fig. 3, for simplicity, the example uses 6×6 visual tokens, the process begins by splitting the image into fixed-size patches and flattening them. Each patch is then represented by its corresponding semantic descriptor. A descriptor can be as simple as a semantic label (*e.g.*, "sky," "sand"), a phrase (*e.g.*, "brown dog", "black dog"), or even a more complex textual description (*e.g.*, "a dog in the left") for intricate scenes. This approach encodes an image into a sequence of semantic descriptors of length 256, which meets the requirements for integrating image segmentation into MLLMs by:

- Adhering to the next-token prediction paradigm of MLLMs, facilitating easier optimization.
- Requiring no architectural changes, ensuring seamless integration and scalability.
- Adopting a text-as-mask paradigm, fully using the text generation capabilities of LLMs for segmentation.

Figure 3: An illustration of semantic descriptors for images and two token compression techniques.

Row-wise RLE. One of the key limitations of full-length semantic descriptors is the long token length due to the inherent spatial redundancy in images. For instance, the average token length of 256 semantic descriptors on the refCOCO (Kazemzadeh et al., 2014) dataset is 583, requiring approximately 19s on a V100 GPU for a single round of referring expression segmentation. To address this issue, we introduce the simple Run-Length Encoding (RLE) (Golomb, 1966) to compress the adjacent repeated texts in semantic descriptors.

A straight forward approach is to directly apply RLE to the whole semantic descriptors, referred as Image-wise RLE (I-RLE). However, we empirically found that it results in a notable performance drop, suggesting that the compressed descriptors may lose crucial spatial information.

To mitigate this issue, we propose a novel Row-wise Run-Length Encoding (R-RLE) technique. As shown in Fig. 3, R-RLE operates at the row level, with each row separated by "\n". This approach reduces the token length from 583 to 154 on average while preserving more spatial information. Importantly, R-RLE demonstrates no performance degradation compared to the full-length semantic descriptors, and significantly enhances the inference speed.

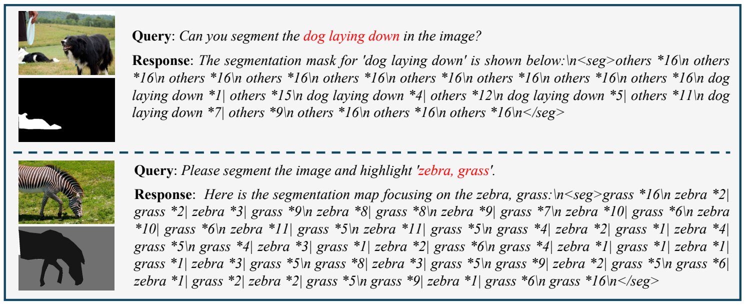

Figure 4: Visual instruction data.

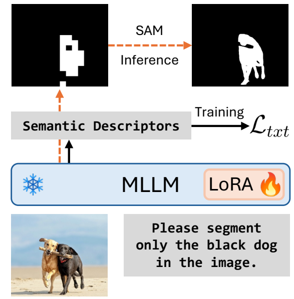

Figure 5: Text4Seg.

3.3 Visual Instruction Tuning of Text4Seg

Building on the proposed semantic descriptors, we construct visual instruction data by leveraging existing segmentation datasets. Fig. 4 shows examples for referring expression segmentation and semantic segmentation. Given a pair of <image, mask>, we resize the mask to a 16×16 resolution and flatten it. The indexes in the sequence are then replaced with their corresponding text labels to create full-length semantic descriptors. We further apply R-RLE to compress the sequence, with descriptors separated by "|" and rows separated by "\n". Finally, the image, text labels, and semantic descriptors are embedded into a query-response template like

Query: `<IMAGE> Can you segment the <text labels> in the image?`
Response: `The result is :\n <seg>semantic descriptors</seg>.`

Note that `<seg>` and `</seg>` are start and end of semantic descriptors.

With such pure text response, Text4Seg can be seamlessly integrated with existing MLLMs without any architectural modifications, as shown in Fig. 5. We use Low-Rank Adaptation (LoRA) (Hu et al., 2021), to fine-tune the MLLMs on our visual instruction data, using its original auto-regressive training objective $\mathcal{L}_{txt}$. In contrast to existing models (Lai et al., 2024; Zhang et al., 2024b; Rasheed et al., 2024), which typically rely on Continued Pre-Training (CPT) with large, mixed datasets to fuse the architectures before fine-tuning on specific downstream tasks, we apply Supervised Fine-Tuning (SFT) directly on the downstream tasks. During inference, to obtain a better pixel-level semantic mask, we optionally apply SAM as the mask refiner with the coarse mask as its prompt.

4 Experiments

4.1 Implementation Details

Model architectures. Our method is built upon several open-source MLLMs, including LLaVA-1.5 (Liu et al., 2024a), DeepseekVL (Lu et al., 2024), InternVL2 (Chen et al., 2024), and Qwen-VL (Bai et al., 2023). The main experiments cover 6 MLMMs with model sizes ranging from 1.3B to 13B parameters, and 3 connectors, including MLP (LLaVA-1.5, DeepseekVL), Pixel Shuffle + MLP (InternVL2) and Cross-attention (Qwen-VL). All architectures were left unaltered during the experiments. Additionally, we employ the off-the-shelf SAM with ViT-H as our mask refiner.

Model training. Our method is implemented using SWIFT (Zhao et al., 2024). All models are trained on 8 Tesla A800 GPUs (40GB) with a global batch size of 128. We use the AdamW optimizer (Loshchilov, 2017), starting with an initial learning rate of 2e-4, which follows a linear decay schedule after a warm-up phase with a ratio of 0.03. The weight decay is set to 0, and gradient norms are clipped at 1.0. To minimize GPU memory usage, we fine-tune all models using LoRA with a rank of 64, along with ZeRO-2 stage memory optimization.

4.2 Referring Expression Segmentation

Settings. For referring expression segmentation (RES), we follow standard evaluation protocols (Lai et al., 2024; Xia et al., 2024) and assess our method using the refCOCO series. We construct

Table 1: **Referring Expression Segmentation** results (cIoU) on refCOCO (+/g) datasets (Kazemzadeh et al., 2014; Mao et al., 2016). GLaMM is depicted in a lighter color as it uses a training dataset two orders of magnitude larger than ours.

Methods	LLM	refCOCO			refCOCO+			refCOCOg		Avg.
		val	testA	testB	val	testA	testB	val	test	
Specialised Segmentation Models										
LAVT (Yang et al., 2022)		72.7	75.8	68.8	62.1	68.4	55.1	61.2	62.1	65.8
ReLA (Liu et al., 2023a)		73.8	76.5	70.2	66.0	71.0	57.7	65.0	66.0	68.3
HIPIE (Wang et al., 2024b)		78.3	-	-	66.2	-	-	69.8	-	-
PolyFormer-L (Liu et al., 2023b)		76.0	78.3	73.3	69.3	74.6	61.9	69.2	70.2	71.6
UNINEXT-L (Yan et al., 2023)		80.3	82.6	77.8	70.0	74.9	62.6	73.4	73.7	74.4
Generalist Segmentation Models ($\leq 8B$)										
NEXT-Chat (Zhang et al., 2023)	Vicuna-7B	74.7	78.9	69.5	65.1	71.9	56.7	67.0	67.0	68.9
LISA (Lai et al., 2024)	Vicuna-7B	74.9	79.1	72.3	65.1	70.8	58.1	67.9	70.6	69.9
PixelLM (Ren et al., 2024)	Vicuna-7B	73.0	76.5	68.2	66.3	71.7	58.3	69.3	70.5	69.2
AnyRef (He et al., 2024)	LLaMA2-7B	76.9	79.9	74.2	70.3	73.5	61.8	70.0	70.7	72.2
GSVA (Xia et al., 2024)	Vicuna-7B	77.2	78.9	73.5	65.9	69.6	59.8	72.7	73.3	71.4
LaSagnA (Wei et al., 2024)	Vicuna-7B	76.8	78.7	73.8	66.4	70.6	60.1	70.6	71.9	71.1
Groundhog (Zhang et al., 2024b)	LLaMA2-7B	78.5	79.9	75.7	70.5	75.0	64.9	74.1	74.6	74.2
GLaMM (Rasheed et al., 2024)	Vicuna-7B	79.5	83.2	76.9	72.6	78.7	64.6	74.2	74.9	75.6
Text4Seg $_{\text{DeepseekVL-1.3B}}$	DeepSeek-1.3B	75.0	78.6	70.1	68.4	73.4	60.0	71.5	71.7	71.1
Text4Seg $_{\text{DeepseekVL-7B}}$	DeepSeek-7B	78.8	81.5	74.9	72.5	77.4	65.9	74.3	74.4	75.0
Text4Seg $_{\text{LLaVA-1.5-7B}}$	Vicuna-7B	**79.3**	**81.9**	**76.2**	72.1	77.6	66.1	72.1	73.9	74.9
Text4Seg $_{\text{Qwen-VL-7B}}$	Qwen-7B	78.0	80.9	74.6	71.6	77.3	66.0	**74.8**	74.7	74.7
Text4Seg $_{\text{InternVL2-8B}}$	InternLM2.5-7B	79.2	81.7	75.6	**72.8**	**77.9**	**66.5**	74.0	**75.3**	**75.4**
Generalist Segmentation Models (13B)										
LISA (Lai et al., 2024)	Vicuna-13B	76.0	78.8	72.9	65.0	70.2	58.1	69.5	70.5	70.1
GSVA (Xia et al., 2024)	Vicuna-13B	78.2	80.4	74.2	67.4	71.5	60.9	**74.2**	**75.6**	72.8
Text4Seg $_{\text{LLaVA-1.5-13B}}$	Vicuna-13B	**80.2**	**82.7**	**77.3**	**73.7**	**78.6**	**67.6**	74.0	75.1	**76.2**

Table 2: **Generalized Referring Expression Segmentation** results on the grefCOCO dataset (Liu et al., 2023a).

Methods	LLM	Validation Set		Test Set A		Test Set B		Avg.
		gIoU	cIoU	gIoU	cIoU	gIoU	cIoU	
Specialised Segmentation Models								
LAVT (Yang et al., 2022)		58.4	57.6	65.9	65.3	55.8	55.0	59.7
ReLA (Liu et al., 2023a)		63.6	62.4	70.0	69.3	61.0	59.9	64.4
Generalist Segmentation Models ($\leq 8B$)								
LISA (Lai et al., 2024)	Vicuna-7B	61.6	61.8	66.3	68.5	58.8	60.6	62.9
GSVA (Xia et al., 2024)	Vicuna-7B	66.5	63.3	71.1	69.9	62.2	60.5	65.6
Text4Seg $_{\text{DeepseekVL-1.3B}}$	DeepSeek-1.3B	69.9	63.2	69.7	67.5	62.3	59.8	65.4
Text4Seg $_{\text{DeepseekVL-7B}}$	DeepSeek-7B	**74.7**	69.0	74.3	73.0	67.4	66.3	70.8
Text4Seg $_{\text{LLaVA-1.5-7B}}$	Vicuna-7B	73.6	67.9	74.1	72.8	66.1	64.8	69.9
Text4Seg $_{\text{Qwen-VL-7B}}$	Qwen-7B	74.4	68.1	73.1	71.5	66.7	65.3	69.9
Text4Seg $_{\text{InternVL2-8B}}$	InternLM2.5-7B	74.4	**69.1**	**75.1**	**73.8**	**67.3**	**66.6**	**71.1**
Generalist Segmentation Models (13B)								
LISA (Lai et al., 2024)	Vicuna-13B	63.5	63.0	68.2	69.7	61.8	62.2	64.7
GSVA (Xia et al., 2024)	Vicuna-13B	68.0	64.1	71.8	70.5	63.8	61.3	66.6
Text4Seg $_{\text{LLaVA-1.5-13B}}$	Vicuna-13B	**74.8**	**69.8**	**75.1**	**74.3**	**68.0**	**67.1**	**71.5**

the referring segmentation dataset by combining the `train` split of refCLEF, refCOCO, refCOCO+ (Kazemzadeh et al., 2014), and refCOCOg (Mao et al., 2016), resulting in a dataset of 800k samples. Our model is trained on this dataset for 5 epochs. Additionally, to evaluate the performance on a multi-object/non-object segmentation task, we construct a generalized referring expression segmentation dataset with 419k samples using the `train` split of grefCOCO (Liu et al., 2023a). We continue to fine-tune the model for 2 epochs.

Result of single object. As summarized in Tab. 1, our Text4Seg achieves the highest performance across all splits of the refCOCO (+/g) datasets. For 7B-scale MLLMs, Text4Seg $_{\text{DeepseekVL-7B}}$ delivers an impressive average cIoU of 75.0, surpassing the closest competitor, Groundhog, which scores

Table 3: **Referring Expression Comprehension** results (Acc@0.5) on RefCOCO (+/g) datasets (Kazemzadeh et al., 2014; Mao et al., 2016).

Methods	LLM	refCOCO			refCOCO+			refCOCOg		Avg.
		val	testA	testB	val	testA	testB	val	test	
Specialised Segmentation Models										
MDETR (Kamath et al., 2021)		86.8	89.6	81.4	79.5	84.1	70.6	81.6	80.9	81.8
G-DINO (Liu et al., 2023c)		90.6	93.2	88.2	82.8	89.0	75.9	86.1	87.0	86.6
PolyFormer-L (Liu et al., 2023b)		90.4	92.9	87.2	85.0	89.8	78.0	85.8	85.9	86.9
UNINEXT-L (Yan et al., 2023)		91.4	93.7	88.9	83.1	87.9	76.2	86.9	87.5	87.0
Generalist Segmentation Models ($\leq$ 8B)										
Shikra (Chen et al., 2023a)	Vicuna-7B	87.0	90.6	80.2	81.6	87.4	72.1	82.3	82.2	82.9
Ferret (You et al., 2023)	Vicuna-7B	87.5	91.4	82.5	80.8	87.4	73.1	83.9	84.8	83.9
Qwen-VL (Bai et al., 2023)	Qwen-7B	88.6	92.3	84.5	82.8	88.6	76.8	86.0	86.3	85.7
InternVL2-8B (Chen et al., 2024)	InternLM2.5-7B	87.1	91.1	80.7	79.8	87.9	71.4	82.7	82.7	82.9
LISA (Lai et al., 2024)	Vicuna-7B	85.4	88.8	82.6	74.2	79.5	68.4	79.3	80.4	79.8
GSVA (Xia et al., 2024)	Vicuna-7B	86.3	89.2	83.8	72.8	78.8	68.0	81.6	81.8	80.3
NEXT-Chat (Zhang et al., 2023)	Vicuna-7B	85.5	90.0	77.9	77.2	84.5	68.0	80.1	79.8	80.4
PixelLM (Ren et al., 2024)	Vicuna-7B	89.8	92.2	86.4	83.2	87.0	78.9	84.6	86.0	86.0
Groma (Ma et al., 2024)	Vicuna-7B	89.5	92.1	86.3	83.9	88.9	78.1	**86.4**	**87.0**	86.5
Text4Seg $_{\text{DeepseekVL-1.3B}}$	DeepSeek-1.3B	86.4	90.3	81.7	80.5	86.3	72.3	82.4	82.7	82.8
Text4Seg $_{\text{DeepseekVL-7B}}$	DeepSeek-7B	89.6	93.3	85.4	84.2	**90.2**	78.5	84.4	84.7	86.3
Text4Seg $_{\text{LLaVA-1.5-7B}}$	Vicuna-7B	**90.8**	**93.7**	**87.6**	84.7	**90.2**	79.0	84.8	85.0	87.0
Text4Seg $_{\text{Qwen-VL-7B}}$	Qwen-7B	89.7	93.0	85.8	84.6	90.1	78.6	85.0	85.1	86.5
Text4Seg $_{\text{InternVL2-8B}}$	InternLM2.5-7B	90.3	93.4	87.5	**85.2**	89.9	**79.5**	85.4	85.4	**87.1**
Generalist Segmentation Models (13B)										
Shikra (Chen et al., 2023a)	Vicuna-13B	87.8	91.1	81.8	82.9	87.8	74.4	82.6	83.2	84.0
LISA (Lai et al., 2024)	Vicuna-13B	85.9	89.1	83.2	74.9	81.1	68.9	80.1	81.5	80.6
GSVA (Xia et al., 2024)	Vicuna-13B	87.7	90.5	84.6	76.5	81.7	70.4	83.9	84.9	82.5
Text4Seg $_{\text{LLaVA-1.5-13B}}$	Vicuna-13B	**91.2**	**94.3**	**88.0**	**85.7**	**90.8**	**80.1**	**85.6**	**85.5**	**87.7**

74.2 cIoU. Notably, Text4Seg $_{\text{InternVL2-8B}}$ stands out with an average of 75.4 cIoU. At the 13B parameter scale, Text4Seg $_{\text{LLaVA-1.5-13B}}$ achieves a marked improvement, with an average cIoU of 76.2, significantly outperforming GSVA's 72.8 cIoU. These results demonstrate the clear advantage of Text4Seg in single-object referring expression segmentation.

Result of multi-/no object. As shown in Tab. 2, Text4Seg maintains its competitive edge in multi-object and no-object referring expression segmentation tasks. For instance, at the 7B scale, Text4Seg records average scores between 69.9 and 71.1, a notable improvement over GSVA's 65.6 on the gRefCOCO dataset. At the 13B scale, Text4Seg $_{\text{LLaVA-1.5-13B}}$ further extends its lead, achieving an average score of 71.5, outperforming GSVA by 4.9 points. These outcomes highlight the robustness and versatility of Text4Seg in handling more complex segmentation challenges.

4.3 Referring Expression Comprehension

Settings. Our Text4Seg can also be directly applied in object detection with a simple *mask2box* paradigm, which first generates a segmentation mask based on the input and then derives the bounding box from the mask. We employ this method to evaluate the referring expression comprehension of our model using the same datasets as in RES. Specifically, a prediction is considered correct if the IoU between the predicted and ground truth bounding boxes exceeds 0.5.

Results. As shown in Tab. 3, our Text4Seg achieves the best results on the refCOCO and refCOCO+ datasets, while Groma performs well on refCOCOg. However, Text4Seg $_{\text{InternVL2-8B}}$ delivers the highest overall accuracy, reaching 87.1%. Notably, both Text4Seg $_{\text{InternVL2-8B}}$ and Text4Seg $_{\text{Qwen-VL-7B}}$ surpass their respective MLLM baselines. In particular, Text4Seg $_{\text{InternVL2-8B}}$ demonstrates a significant improvement over InternVL2-8B, increasing its average accuracy from 82.9% to 87.1%. Additionally, our Text4Seg $_{\text{LLaVA-1.5-13B}}$ outperforms previous SOTA, Shikra, by an average margin of 3.7%. These results highlight the superiority of our Text4Seg, which offers a finer, pixel-level representation that enhances the precision of bounding box predictions.

Table 4: Results on **visual question answering** and **RES** benchmarks. Note: refC denotes refCOCO; Mix[†] is a combination of referring segmentation, semantic segmentation and VQA datasets from LISA.

Methods	Training Data	VQA						RES (val)		
		VQAv2	GQA	VisWiz	ScienceQA	TextQA	POPE	refC	refC+	refCg
LISA	Mix[†]	-	-	-	-	-	-	74.1	62.4	66.4
LLaVA-1.5	665k	78.0	61.7	50.6	68.4	55.0	85.4	-	-	-
Text4Seg	665k + refseg	76.6	60.2	50.9	68.1	55.0	84.2	77.5	70.7	73.4

4.4 Visual Understanding

Settings. Our text-as-mask paradigm allows for seamless integration of downstream segmentation task into the pre-training of MLLMs. To evaluate its effectiveness, we assess the model's performance on various visual understanding benchmarks, using the LLaVA-1.5-7B model as the baseline. Our method, Text4Seg, built upon the stage-2 of LLaVA-1.5-7B, is trained on both the LLaVA-v1.5-mix665k dataset and our referring segmentation datasets. For a comprehensive comparison, we also report the performance of the LLaVA-1.5-7B model based on our implementation.

Results. Table 4 presents a comparison between LLaVA-1.5 and Text4Seg across various VQA and RES benchmarks. Text4Seg, trained on the mixed dataset, not only achieves performance comparable to LLaVA-1.5 in visual question answering tasks, but also demonstrates strong results in RES benchmarks. These results validate that our text generation based segmentation method acts as a seamless enhancement, offering a streamlined approach for pre-training MLLMs. It successfully integrates robust segmentation functionality without compromising the model's conversational capabilities.

4.5 Open Vocabulary Segmentation

Settings. We follow LaSagnA (Wei et al., 2024) to evaluate the performance of Text4Seg on open-vocabulary segmentation tasks. Our Text4Seg is built upon LLaVA-1.5-7B and trained on the COCOStuff (Caesar et al., 2018) for 1 epoch. We evaluate the model's performance on ADE20K (A-150) (Zhou et al., 2019), PASCAL Context 59 (PC-59) (Mottaghi et al., 2014), and PASCAL VOC 20 (PAS-20) (Everingham, 2009) datasets, using mIoU as the evaluation metric.

Table 5: **Open Vocabulary Segmentation** results (mIoU) on various segmentation datasets.

Methods	A-150	PC-59	PAS-20
Specialised Segmentation Models			
ClearCLIP	16.7	35.9	80.9
ProxyCLIP	24.2	39.6	83.3
MaskCLIP	23.7	45.9	-
GroupViT	9.2	23.4	79.7
OVSeg	24.8	53.3	92.6
SAN	27.5	53.8	94.0
Generalist Segmentation Models (7B)			
LaSagnA	14.3	46.1	69.8
Text4Seg	**16.5**	**52.5**	**76.5**

Results. As reported in the Tab. 5, it is expected that Text4Seg falls behind specialized segmentation models (*e.g.*, ClearCLIP (Lan et al., 2024a), ProxyCLIP (Lan et al., 2024b), MaskCLIP (Ding et al., 2022), GroupViT (Xu et al., 2022), OVSeg (Liang et al., 2023), and SAN (Xu et al., 2023)), because LLMs typically require quite large datasets to be sufficiently trained. However, Text4Seg still demonstrates competitive performance on the PC-59 benchmark, underscoring its efficiency. More importantly, it significantly outperforms the MLLM-based LaSagnA, which uses an additional decoder, showcasing its strong potential for open-vocabulary segmentation.

4.6 Ablation Study

Given that the focus of this work is on introducing semantic descriptors for visual segmentation and grounding, we conducted a series of ablation studies to assess the impact of semantic descriptors on performance, using InternVL2-8B (Chen et al., 2024) as the MLLM.

Resolution of semantic descriptors. To analyze the impact of varying the resolution of semantic descriptors on RES performance, we create instruction-tuning datasets with different densities of

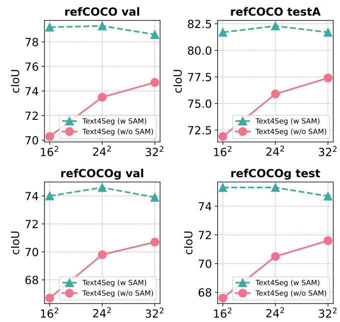

Figure 6: RES comparison across different resolutions.

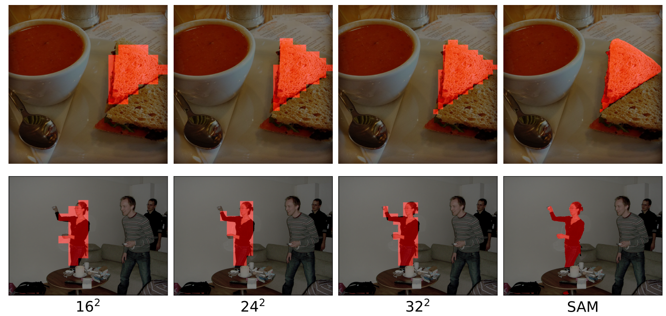

Figure 7: Visualization of RES results across different resolutions, and with SAM as mask refiner.

Table 6: Ablation study of mask refiner on refCOCO val.

Method	Refiner	cIoU	Acc@0.5	Time (s)
Text4Seg	None	73.5	89.3	5.34
Text4Seg	SAM-B	75.5	89.9	5.54
Text4Seg	SAM-L	79.1	90.6	5.73
Text4Seg	SAM-H	79.2	90.0	5.92

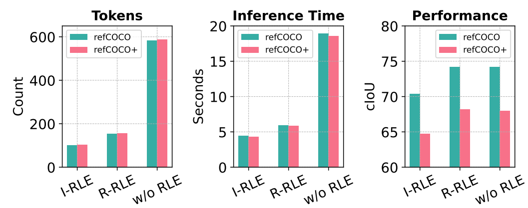

Figure 8: R-RLE is better than I-RLE.

semantic descriptors. Specifically, we represent each image with 16×16, 24×24, and 32×32 semantic descriptors to explore how finer or coarser resolutions affect model accuracy. As shown in Fig. 6, the performance of Text4Seg without a mask refiner improves with higher resolution, from 67.5 cIoU at 16^2 to 71.4 cIoU at 32^2 on average, surpassing LISA at 69.9 cIoU. Two examples are illustrated in Fig. 7. *Note that the improvement is achieved without increasing the feature resolution from the vision tower of MLLM.* While higher-density semantic descriptors improve results, it also significantly increases token length and computational cost. Therefore, we incorporate an off-the-shelf SAM to refine the outputs. Experimental results show that using 16^2 semantic descriptors with SAM already achieves optimal performance.

Mask refiner with SAM variants. Tab. 6 compares the performance of various mask refiners, such as SAM with different architectures, against no refiner for semantic descriptors at a 16×16 resolution. SAM with the ViT-L architecture achieves similar performance to SAM with ViT-H while reducing inference time. Notably, Text4Seg with SAM-L increases the average performance on RES tasks from 73.5 to 79.1 cIoU compared to Text4Seg without a mask refiner, with only a little increase in inference time.

I-RLE v.s. R-RLE. We investigate the impact of different encoding methods for semantic descriptors at a 16×16 resolution using the `train/val` splits of the refCOCO and refCOCO+ datasets. As illustrated in Fig. 8, while full-length semantic descriptors achieve high performance, they suffer from significantly longer inference times (∼19 seconds) due to longer output tokens (∼590) on both datasets. Although the I-RLE method reduces both the number of tokens and inference time, it results in a notable performance drop, from 74.2 to 70.4 cIoU on refCOCO and 68.0 to 64.7 cIoU on refCOCO+. Our proposed R-RLE method strikes a better balance, reducing the length of semantic descriptors by 74% and improving inference speed by an average of 3×, while still maintaining the same performance.

4.7 Visualization Examples

We present qualitative comparisons between Text4Seg and GSVA in Figs. 9 and 10. In the single-object RES task, Text4Seg demonstrates a superior understanding of referring expressions, generating more accurate and precise segmentation maps compared to GSVA. In the GRES task (Fig. 10), GSVA tends to incorrectly segment empty objects despite the inclusion of a <REJ> token (as seen

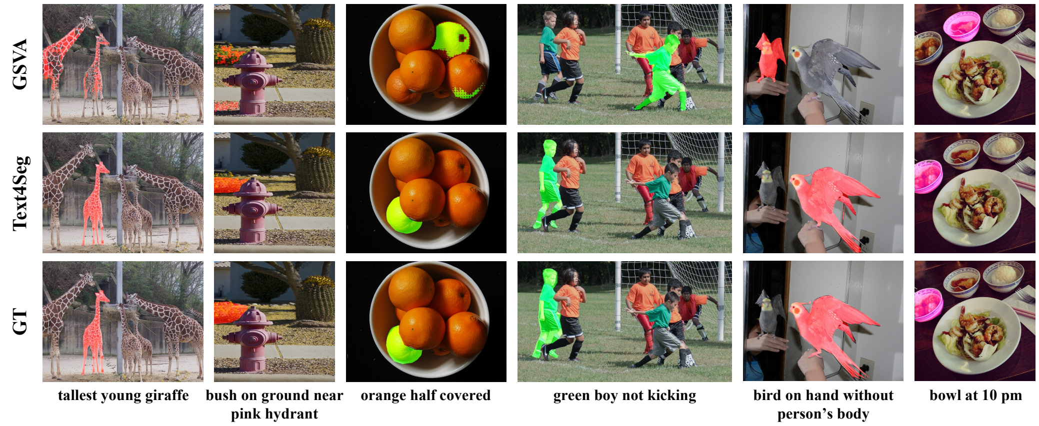

Figure 9: Visualizations of Text4Seg and GSVA (Xia et al., 2024) on the RES task. Our Text4Seg is based on InternVL2 backbone. The corresponding referring expressions are displayed in the bottom.

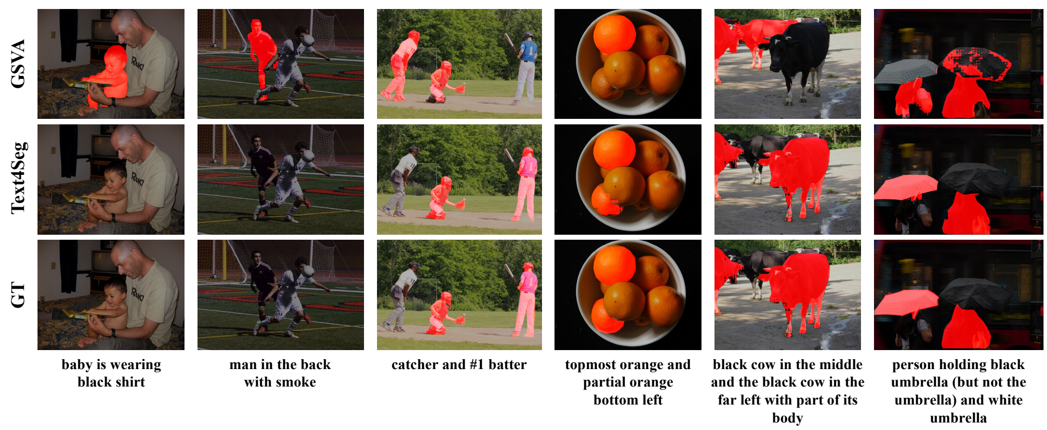

Figure 10: Visualizations of Text4Seg and GSVA (Xia et al., 2024) on the GRES task.

in the first two columns). In contrast, Text4Seg consistently avoids such mistakes by labeling them as "`others`" without special design. Furthermore, Text4Seg significantly outperforms GSVA in the multiple-object RES task, delivering more precise segmentation results with better grounding performance. These results fully validate the effectiveness of Text4Seg in handling diverse and challenging visual grounding and segmentation tasks.

5 Conclusion

In this work, we present Text4Seg, a decoder-free framework that integrates seamlessly with existing MLLMs for image segmentation using a novel *text-as-mask* paradigm. With the novel semantic descriptors, Text4Seg achieves state-of-the-art performance across various segmentation tasks, without requiring architecture modifications. We further introduce the Row-wise Run-Length Encoding (R-RLE) to compress semantic descriptors, which significantly improves the efficiency of Text4Seg while maintaining the performance. In summary, this work highlights the flexibility and effectiveness of Text4Seg in bridging the gap between MLLMs and vision-centric tasks, offering a scalable solution for future research in multimodal learning.

References

Jean-Baptiste Alayrac, Jeff Donahue, Pauline Luc, Antoine Miech, Iain Barr, Yana Hasson, Karel Lenc, Arthur Mensch, Katherine Millican, Malcolm Reynolds, et al. Flamingo: a visual language model for few-shot learning. *Advances in neural information processing systems*, 35:23716–23736, 2022. 3

Anas Awadalla, Irena Gao, Josh Gardner, Jack Hessel, Yusuf Hanafy, Wanrong Zhu, Kalyani Marathe, Yonatan Bitton, Samir Gadre, Shiori Sagawa, et al. Openflamingo: An open-source framework for training large autoregressive vision-language models. *arXiv preprint arXiv:2308.01390*, 2023. 3

Jinze Bai, Shuai Bai, Shusheng Yang, Shijie Wang, Sinan Tan, Peng Wang, Junyang Lin, Chang Zhou, and Jingren Zhou. Qwen-vl: A versatile vision-language model for understanding, localization, text reading, and beyond. *arXiv preprint arXiv:2308.12966*, 2023. 1, 2, 3, 5, 7

Holger Caesar, Jasper Uijlings, and Vittorio Ferrari. Coco-stuff: Thing and stuff classes in context. In *Proceedings of the IEEE conference on computer vision and pattern recognition*, pp. 1209–1218, 2018. 8

Keqin Chen, Zhao Zhang, Weili Zeng, Richong Zhang, Feng Zhu, and Rui Zhao. Shikra: Unleashing multimodal llm's referential dialogue magic. *arXiv preprint arXiv:2306.15195*, 2023a. 7, 22

Ting Chen, Saurabh Saxena, Lala Li, David J Fleet, and Geoffrey Hinton. Pix2seq: A language modeling framework for object detection. *arXiv preprint arXiv:2109.10852*, 2021. 3

Zhe Chen, Jiannan Wu, Wenhai Wang, Weijie Su, Guo Chen, Sen Xing, Muyan Zhong, Qinglong Zhang, Xizhou Zhu, Lewei Lu, Bin Li, Ping Luo, Tong Lu, Yu Qiao, and Jifeng Dai. Internvl: Scaling up vision foundation models and aligning for generic visual-linguistic tasks. *arXiv preprint arXiv:2312.14238*, 2023b. 2

Zhe Chen, Weiyun Wang, Hao Tian, Shenglong Ye, Zhangwei Gao, Erfei Cui, Wenwen Tong, Kongzhi Hu, Jiapeng Luo, Zheng Ma, et al. How far are we to gpt-4v? closing the gap to commercial multimodal models with open-source suites. *arXiv preprint arXiv:2404.16821*, 2024. 1, 5, 7, 8

Wenliang Dai, Junnan Li, Dongxu Li, Anthony Tiong, Junqi Zhao, Weisheng Wang, Boyang Li, Pascale Fung, and Steven Hoi. InstructBLIP: Towards general-purpose vision-language models with instruction tuning. In *Thirty-seventh Conference on Neural Information Processing Systems*, 2023. URL https://openreview.net/forum?id=vvoWPYqZJA. 3

Zheng Ding, Jieke Wang, and Zhuowen Tu. Open-vocabulary universal image segmentation with maskclip. *arXiv preprint arXiv:2208.08984*, 2022. 8

Alexey Dosovitskiy, Lucas Beyer, Alexander Kolesnikov, Dirk Weissenborn, Xiaohua Zhai, Thomas Unterthiner, Mostafa Dehghani, Matthias Minderer, Georg Heigold, Sylvain Gelly, Jakob Uszkoreit, and Neil Houlsby. An image is worth 16x16 words: Transformers for image recognition at scale. In *International Conference on Learning Representations*, 2021. URL https://openreview.net/forum?id=YicbFdNTTy. 2, 4

Mark Everingham. The pascal visual object classes challenge 2007. In *http://www. pascal-network. org/challenges/VOC/voc2007/workshop/index. html*, 2009. 8

Hao Fei, Shengqiong Wu, Hanwang Zhang, Tat-Seng Chua, and Shuicheng Yan. Vitron: A unified pixel-level vision llm for understanding, generating, segmenting, editing, 2024. 3

Solomon Golomb. Run-length encodings (corresp.). *IEEE transactions on information theory*, 12 (3):399–401, 1966. 4

Junwen He, Yifan Wang, Lijun Wang, Huchuan Lu, Jun-Yan He, Jin-Peng Lan, Bin Luo, and Xuansong Xie. Multi-modal instruction tuned llms with fine-grained visual perception. In *Proceedings of the IEEE/CVF Conference on Computer Vision and Pattern Recognition*, pp. 13980–13990, 2024. 1, 6

Edward J Hu, Yelong Shen, Phillip Wallis, Zeyuan Allen-Zhu, Yuanzhi Li, Shean Wang, Lu Wang, and Weizhu Chen. Lora: Low-rank adaptation of large language models. *arXiv preprint arXiv:2106.09685*, 2021. 5

Wu Jiannan, Zhong Muyan, Xing Sen, Lai Zeqiang, Liu Zhaoyang, Chen Zhe, Wang Wenhai, Zhu Xizhou, Lu Lewei, Lu Tong, Luo Ping, Qiao Yu, and Dai Jifeng. Visionllm v2: An end-to-end generalist multimodal large language model for hundreds of vision-language tasks. *arXiv preprint arXiv:2406.08394*, 2024. 1, 3

Aishwarya Kamath, Mannat Singh, Yann LeCun, Gabriel Synnaeve, Ishan Misra, and Nicolas Carion. Mdetr-modulated detection for end-to-end multi-modal understanding. In *Proceedings of the IEEE/CVF international conference on computer vision*, pp. 1780–1790, 2021. 7

Sahar Kazemzadeh, Vicente Ordonez, Mark Matten, and Tamara Berg. Referitgame: Referring to objects in photographs of natural scenes. In *Proceedings of the 2014 conference on empirical methods in natural language processing (EMNLP)*, pp. 787–798, 2014. 4, 6, 7

Alexander Kirillov, Eric Mintun, Nikhila Ravi, Hanzi Mao, Chloe Rolland, Laura Gustafson, Tete Xiao, Spencer Whitehead, Alexander C Berg, Wan-Yen Lo, et al. Segment anything. In *Proceedings of the IEEE/CVF International Conference on Computer Vision*, pp. 4015–4026, 2023. 1, 3

Xin Lai, Zhuotao Tian, Yukang Chen, Yanwei Li, Yuhui Yuan, Shu Liu, and Jiaya Jia. Lisa: Reasoning segmentation via large language model. In *Proceedings of the IEEE/CVF Conference on Computer Vision and Pattern Recognition*, pp. 9579–9589, 2024. 1, 2, 3, 5, 6, 7, 21, 22

Mengcheng Lan, Chaofeng Chen, Yiping Ke, Xinjiang Wang, Litong Feng, and Wayne Zhang. Clearclip: Decomposing clip representations for dense vision-language inference. In *ECCV*, 2024a. 8

Mengcheng Lan, Chaofeng Chen, Yiping Ke, Xinjiang Wang, Litong Feng, and Wayne Zhang. Proxyclip: Proxy attention improves clip for open-vocabulary segmentation. In *ECCV*, 2024b. 8

Bo Li, Yuanhan Zhang, Liangyu Chen, Jinghao Wang, Jingkang Yang, and Ziwei Liu. Otter: A multi-modal model with in-context instruction tuning. *arXiv preprint arXiv:2305.03726*, 2023a. 3

Bo Li, Yuanhan Zhang, Dong Guo, Renrui Zhang, Feng Li, Hao Zhang, Kaichen Zhang, Yanwei Li, Ziwei Liu, and Chunyuan Li. Llava-onevision: Easy visual task transfer. *arXiv preprint arXiv:2408.03326*, 2024a. 2, 3

Junnan Li, Dongxu Li, Silvio Savarese, and Steven Hoi. Blip-2: Bootstrapping language-image pre-training with frozen image encoders and large language models. In *International conference on machine learning*, pp. 19730–19742. PMLR, 2023b. 3

Yanwei Li, Yuechen Zhang, Chengyao Wang, Zhisheng Zhong, Yixin Chen, Ruihang Chu, Shaoteng Liu, and Jiaya Jia. Mini-gemini: Mining the potential of multi-modality vision language models. *arXiv preprint arXiv:2403.18814*, 2024b. 3

Zhang Li, Biao Yang, Qiang Liu, Zhiyin Ma, Shuo Zhang, Jingxu Yang, Yabo Sun, Yuliang Liu, and Xiang Bai. Monkey: Image resolution and text label are important things for large multi-modal models. In *Proceedings of the IEEE/CVF Conference on Computer Vision and Pattern Recognition*, pp. 26763–26773, 2024c. 3

Feng Liang, Bichen Wu, Xiaoliang Dai, Kunpeng Li, Yinan Zhao, Hang Zhang, Peizhao Zhang, Peter Vajda, and Diana Marculescu. Open-vocabulary semantic segmentation with mask-adapted clip. In *Proceedings of the IEEE/CVF Conference on Computer Vision and Pattern Recognition*, pp. 7061–7070, 2023. 8

Ziyi Lin, Chris Liu, Renrui Zhang, Peng Gao, Longtian Qiu, Han Xiao, Han Qiu, Chen Lin, Wenqi Shao, Keqin Chen, et al. Sphinx: The joint mixing of weights, tasks, and visual embeddings for multi-modal large language models. *arXiv preprint arXiv:2311.07575*, 2023. 3

Chang Liu, Henghui Ding, and Xudong Jiang. Gres: Generalized referring expression segmentation. In *Proceedings of the IEEE/CVF conference on computer vision and pattern recognition*, pp. 23592–23601, 2023a. 6

Haotian Liu, Chunyuan Li, Yuheng Li, and Yong Jae Lee. Improved baselines with visual instruction tuning. In *Proceedings of the IEEE/CVF Conference on Computer Vision and Pattern Recognition*, pp. 26296–26306, 2024a. 1, 3, 5

Haotian Liu, Chunyuan Li, Yuheng Li, Bo Li, Yuanhan Zhang, Sheng Shen, and Yong Jae Lee. Llava-next: Improved reasoning, ocr, and world knowledge, 2024b. 3

Haotian Liu, Chunyuan Li, Qingyang Wu, and Yong Jae Lee. Visual instruction tuning. *Advances in neural information processing systems*, 36, 2024c. 1, 3

Jiang Liu, Hui Ding, Zhaowei Cai, Yuting Zhang, Ravi Kumar Satzoda, Vijay Mahadevan, and R Manmatha. Polyformer: Referring image segmentation as sequential polygon generation. In *Proceedings of the IEEE/CVF Conference on Computer Vision and Pattern Recognition*, pp. 18653–18663, 2023b. 6, 7

Shilong Liu, Zhaoyang Zeng, Tianhe Ren, Feng Li, Hao Zhang, Jie Yang, Chunyuan Li, Jianwei Yang, Hang Su, Jun Zhu, et al. Grounding dino: Marrying dino with grounded pre-training for open-set object detection. *arXiv preprint arXiv:2303.05499*, 2023c. 7

I Loshchilov. Decoupled weight decay regularization. *arXiv preprint arXiv:1711.05101*, 2017. 5

Haoyu Lu, Wen Liu, Bo Zhang, Bingxuan Wang, Kai Dong, Bo Liu, Jingxiang Sun, Tongzheng Ren, Zhuoshu Li, Yaofeng Sun, et al. Deepseek-vl: towards real-world vision-language understanding. *arXiv preprint arXiv:2403.05525*, 2024. 1, 2, 5

Chuofan Ma, Yi Jiang, Jiannan Wu, Zehuan Yuan, and Xiaojuan Qi. Groma: Localized visual tokenization for grounding multimodal large language models. *arXiv preprint arXiv:2404.13013*, 2024. 1, 7

Junhua Mao, Jonathan Huang, Alexander Toshev, Oana Camburu, Alan L Yuille, and Kevin Murphy. Generation and comprehension of unambiguous object descriptions. In *Proceedings of the IEEE conference on computer vision and pattern recognition*, pp. 11–20, 2016. 6, 7

Roozbeh Mottaghi, Xianjie Chen, Xiaobai Liu, Nam-Gyu Cho, Seong-Whan Lee, Sanja Fidler, Raquel Urtasun, and Alan Yuille. The role of context for object detection and semantic segmentation in the wild. In *Proceedings of the IEEE conference on computer vision and pattern recognition*, pp. 891–898, 2014. 8

Zhiliang Peng, Wenhui Wang, Li Dong, Yaru Hao, Shaohan Huang, Shuming Ma, and Furu Wei. Kosmos-2: Grounding multimodal large language models to the world. *arXiv preprint arXiv:2306.14824*, 2023. 3

Hanoona Rasheed, Muhammad Maaz, Sahal Shaji, Abdelrahman Shaker, Salman Khan, Hisham Cholakkal, Rao M Anwer, Eric Xing, Ming-Hsuan Yang, and Fahad S Khan. Glamm: Pixel grounding large multimodal model. In *Proceedings of the IEEE/CVF Conference on Computer Vision and Pattern Recognition*, pp. 13009–13018, 2024. 1, 3, 5, 6

Zhongwei Ren, Zhicheng Huang, Yunchao Wei, Yao Zhao, Dongmei Fu, Jiashi Feng, and Xiaojie Jin. Pixellm: Pixel reasoning with large multimodal model. In *Proceedings of the IEEE/CVF Conference on Computer Vision and Pattern Recognition*, pp. 26374–26383, 2024. 1, 3, 6, 7

Kunpeng Song, Yizhe Zhu, Bingchen Liu, Qing Yan, Ahmed Elgammal, and Xiao Yang. Moma: Multimodal llm adapter for fast personalized image generation. *arXiv preprint arXiv:2404.05674*, 2024. 1

Wenhai Wang, Zhe Chen, Xiaokang Chen, Jiannan Wu, Xizhou Zhu, Gang Zeng, Ping Luo, Tong Lu, Jie Zhou, Yu Qiao, et al. Visionllm: Large language model is also an open-ended decoder for vision-centric tasks. *Advances in Neural Information Processing Systems*, 36, 2024a. 1, 2, 3

Xudong Wang, Shufan Li, Konstantinos Kallidromitis, Yusuke Kato, Kazuki Kozuka, and Trevor Darrell. Hierarchical open-vocabulary universal image segmentation. *Advances in Neural Information Processing Systems*, 36, 2024b. 6

Zhenyu Wang, Aoxue Li, Zhenguo Li, and Xihui Liu. Genartist: Multimodal llm as an agent for unified image generation and editing. *arXiv preprint arXiv:2407.05600*, 2024c. 1

Cong Wei, Haoxian Tan, Yujie Zhong, Yujiu Yang, and Lin Ma. Lasagna: Language-based segmentation assistant for complex queries. *arXiv preprint arXiv:2404.08506*, 2024. 6, 8, 20

Shengqiong Wu, Hao Fei, Xiangtai Li, Jiayi Ji, Hanwang Zhang, Tat-Seng Chua, and Shuicheng Yan. Towards semantic equivalence of tokenization in multimodal llm. *arXiv preprint arXiv:2406.05127*, 2024. 1, 3

Zhuofan Xia, Dongchen Han, Yizeng Han, Xuran Pan, Shiji Song, and Gao Huang. Gsva: Generalized segmentation via multimodal large language models. In *Proceedings of the IEEE/CVF Conference on Computer Vision and Pattern Recognition*, pp. 3858–3869, 2024. 1, 3, 5, 6, 7, 10, 21, 22

Jiarui Xu, Shalini De Mello, Sifei Liu, Wonmin Byeon, Thomas Breuel, Jan Kautz, and Xiaolong Wang. Groupvit: Semantic segmentation emerges from text supervision. In *Proceedings of the IEEE/CVF Conference on Computer Vision and Pattern Recognition*, pp. 18134–18144, 2022. 8

Mengde Xu, Zheng Zhang, Fangyun Wei, Han Hu, and Xiang Bai. Side adapter network for open-vocabulary semantic segmentation. In *Proceedings of the IEEE/CVF Conference on Computer Vision and Pattern Recognition*, pp. 2945–2954, 2023. 8

Ruyi Xu, Yuan Yao, Zonghao Guo, Junbo Cui, Zanlin Ni, Chunjiang Ge, Tat-Seng Chua, Zhiyuan Liu, Maosong Sun, and Gao Huang. Llava-uhd: an lmm perceiving any aspect ratio and high-resolution images. *arXiv preprint arXiv:2403.11703*, 2024. 3

Bin Yan, Yi Jiang, Jiannan Wu, Dong Wang, Ping Luo, Zehuan Yuan, and Huchuan Lu. Universal instance perception as object discovery and retrieval. In *Proceedings of the IEEE/CVF Conference on Computer Vision and Pattern Recognition*, pp. 15325–15336, 2023. 6, 7

Zhao Yang, Jiaqi Wang, Yansong Tang, Kai Chen, Hengshuang Zhao, and Philip HS Torr. Lavt: Language-aware vision transformer for referring image segmentation. In *Proceedings of the IEEE/CVF Conference on Computer Vision and Pattern Recognition*, pp. 18155–18165, 2022. 6

Qinghao Ye, Haiyang Xu, Jiabo Ye, Ming Yan, Anwen Hu, Haowei Liu, Qi Qian, Ji Zhang, and Fei Huang. mplug-owl2: Revolutionizing multi-modal large language model with modality collaboration. In *Proceedings of the IEEE/CVF Conference on Computer Vision and Pattern Recognition*, pp. 13040–13051, 2024. 3

Shukang Yin, Chaoyou Fu, Sirui Zhao, Ke Li, Xing Sun, Tong Xu, and Enhong Chen. A survey on multimodal large language models. *arXiv preprint arXiv:2306.13549*, 2023. 1, 4

Haoxuan You, Haotian Zhang, Zhe Gan, Xianzhi Du, Bowen Zhang, Zirui Wang, Liangliang Cao, Shih-Fu Chang, and Yinfei Yang. Ferret: Refer and ground anything anywhere at any granularity. *arXiv preprint arXiv:2310.07704*, 2023. 7

Ao Zhang, Liming Zhao, Chen-Wei Xie, Yun Zheng, Wei Ji, and Tat-Seng Chua. Next-chat: An lmm for chat, detection and segmentation. *arXiv preprint arXiv:2311.04498*, 2023. 1, 3, 6, 7

Tao Zhang, Xiangtai Li, Hao Fei, Haobo Yuan, Shengqiong Wu, Shunping Ji, Chen Change Loy, and Shuicheng Yan. Omg-llava: Bridging image-level, object-level, pixel-level reasoning and understanding. *arXiv preprint arXiv:2406.19389*, 2024a. 3

Yichi Zhang, Ziqiao Ma, Xiaofeng Gao, Suhaila Shakiah, Qiaozi Gao, and Joyce Chai. Groundhog: Grounding large language models to holistic segmentation. In *Proceedings of the IEEE/CVF conference on computer vision and pattern recognition*, pp. 14227–14238, 2024b. 1, 3, 5, 6

Yuze Zhao, Jintao Huang, Jinghan Hu, Xingjun Wang, Yunlin Mao, Daoze Zhang, Zeyinzi Jiang, Zhikai Wu, Baole Ai, Ang Wang, Wenmeng Zhou, and Yingda Chen. Swift:a scalable lightweight infrastructure for fine-tuning, 2024. URL `https://arxiv.org/abs/2408.05517`. 5

Bolei Zhou, Hang Zhao, Xavier Puig, Tete Xiao, Sanja Fidler, Adela Barriuso, and Antonio Torralba. Semantic understanding of scenes through the ade20k dataset. *International Journal of Computer Vision*, 127:302–321, 2019. 8

A Additional Implementation Details

A.1 Implementation of adopting SAM as mask refiner.

We employ SAM with a ViT-H architecture as our mask refiner. For referring expression segmentation tasks, we refine the coarse masks produced by Text4Seg from the semantic descriptors using the following process:

- **Step 1:** Convert the binary mask into a logit representation by applying the inverse sigmoid function.
- **Step 2:** Randomly select 10 positive and 10 negative points from the coarse binary mask.
- **Step 3:** Provide the selected points as point prompts, the logit representation as a mask prompt, and the RGB image as input to SAM, generating a refined mask and updated logits.
- **Step 4:** Repeat Step 3 twice.

This iterative process helps enhance the quality of the segmentation mask. The final mask produced by SAM is then resized to the original image dimensions, resulting in pixel-level segmentation masks. For open-vocabulary segmentation, this strategy is applied iteratively across multiple class masks, which are then combined to form the final segmentation maps.

A.2 Details of Training Hyper-parameters

Table 7 presents the training hyperparameters used for training Text4Seg on the referring expression segmentation task. We primarily adhere to the same settings as LLaVA-1.5, and these parameters are consistently applied across other tasks as well.

Table 7: Hyper-parameters and training settings for RES task.

	Param Name	Value
Optimizer	Type	AdamW
	Learning rate	2e-4
	Weight decay	0.0
	(β_1, β_2)	(0.9, 0.95)
	Gradient norm clip	1.0
	Scheduler	Linearly decay
	Warmup ratio	0.03
LoRA	Rank	64
	Alpha (α)	128
	Dropout	0.05
	Module	Linear layers of connector and LLMs
Training	Trainable #Params.	About 2% of the LLM (7B $\rightarrow$ 160M)
	Numerical precision	FP16
	Global batch size	128
	Number of samples per epoch	800k
	Total epochs	5
	GPUs	A800(40G) $\times$ 8
	Time	About 2 Days

B Comparison of training datasets

Most prior methods follow a two-stage training paradigm: **Continued Pre-Training (CPT)** using large datasets, followed by **Supervised Fine-Tuning (SFT)** for specific tasks. The datasets used in these approaches are summarized in the following tables:

- Tab. 8: Datasets for **Continued Pre-Training (CPT)**
- Tab. 9: Datasets for **Supervised Fine-Tuning (SFT)** in **Referring Expression Segmentation (RES)**
- Tab. 10: Datasets for **Supervised Fine-Tuning (SFT)** in **Generalized Referring Expression Segmentation (GRES)**

We can note that:

1. For CPT, previous methods rely heavily on large and diverse datasets, whereas our approach, Text4Seg, eliminates this requirement, demonstrating superior efficiency and effectiveness.
2. For SFT, we ensure a fair comparison by following previous works and train on:
   - The `train` split of refCOCO series for **RES** and **REC** tasks.
   - The `train` split of grefCOCO for the **GRES** task.

Table 8: Training datasets of **Continued Pre-Training (CPT)**.

Methods	**Datasets**
LISA	ADE20K, COCO-Stuff, PACO-LVIS, PartImageNet, PASCAL-Part, refCLEF, refCOCO, refCOCO+, refCOCOg, LLaVA-v1.5-mix665k
PixelLM	ADE20K, COCO-Stuff, PACO-LVIS, refCLEF, refCOCO, refCOCO+, refCOCOg, LLAVA-150k, multi-target reasoning segmentation (MUSE)
GSVA	ADE20K, COCO-Stuff, PACO-LVIS, Mapillary Vistas, PASCAL-Part, refCLEF, refCOCO, refCOCO+, refCOCOg, gRefCOCO, LLaVA-Instruct-150K, ReasonSeg
AnyRef	ADE20K, COCO-Stuff, PACO-LVIS, refCLEF, refCOCO, refCOCO+, refCOCOg, PhraseCut, Flickr30K Entities, AVSBench
NEXT-Chat	Flickr30K Entities, Visual Genome, RefCOCO, RefCOCO+, RefCOCOg, VQAv2, PointQA, Visual7W, VCR, LLaVA-Instruct-150K, VG grounded captioning, Shikra-RD
Groundhog	Multi-Modal Multi-Grained Grounding dataset (M3G2): PNG, Flickr30K-Entity, refCLEF, refCOCO, refCOCO+, refCOCOg, gRefCOCO, PhraseCut, D-Cube, ReasonSeg, RIO, SK-VG, VizWiz-G, TextVQA-X, GQA, VQS, Shikra-BinaryQA, EntityCount, FoodSeg-QA, LVIS-QA, RefCOCO-REG, RefCOCO+-REG, RefCOCOg-REG, gRefCOCO-REG, VG-SpotCap, V7W, PointQA, VCR, ShikraRD, SVIT-RD, Guesswhat, VG-RefMatch, HierText
GLaMM	Grounding-anything Dataset (GranD): **11M** images, **810M** masks, **84M** referring expressions, GranD-f
Text4Seg	**None**

Table 9: Referring Expression Segmentation Datasets of **Supervised Fine-Tuning (SFT)**. † Other methods have already incorporated refCLEF dataset in their CPT training datasets.

Methods	**Datasets**
LISA	refCOCO, refCOCO+, refCOCOg
PixelLM	None
GSVA	refCOCO, refCOCO+, refCOCOg
AnyRef	refCOCO, refCOCO+, refCOCOg
NEXT-Chat	refCOCO, refCOCO+, refCOCOg
Groundhog	None
GLaMM	refCOCO, refCOCO+, refCOCOg
Text4Seg	refCOCO, refCOCO+, refCOCOg, refCLEF†

Table 10: Generalized Referring Expression Segmentation Datasets of **Supervised Fine-Tuning (SFT)**.

Methods	**Datasets**
LISA	grefCOCO
GSVA	grefCOCO
Text4Seg	grefCOCO

C ADDITIONAL VISUAL INSTRUCTION DATA DETAILS

Query-answer template. We provide the question-answer templates in the Figs. 11 to 13. For partial segmentation tasks, the templates are designed to segment **only a subset of objects in the image**, such as a single object in the RES task, multiple objects in the GRES task, or partial labels in semantic segmentation tasks. For conditioned segmentation tasks, the user provides a list of condition labels, and the model segments the entire image based on those specified labels. For open-vocabulary segmentation tasks, the model leverages its open-vocabulary capabilities to segment the image and label all detected categories.

Visual instruction data on RES datasets. We adopt the question-answer templates from Fig. 11 to construct the training data. Specifically, we iterate through all `<image, referring expression, mask>` pairs in the dataset, transforming the vanilla mask into semantic descriptors, using the referring expression as the descriptor. The referring expression is placed in the `[class_name]` placeholder within each question-answer template. The RES training set is constructed by combining the `train` splits of refCLEF, refCOCO, refCOCO+, and refCOCOg, with the process repeated twice. This results in a final RES training set comprising 800k samples. The same method is applied to construct the GRES training set, which contains 419k samples.

Visual instruction data on open-vocabulary segmentation datasets. For the open-vocabulary segmentation task, we utilize all three types of question-answer templates. Specifically, we construct our visual instruction data using the COCOStuff dataset. The ratio of open-vocabulary segmentation templates, partial segmentation templates, and conditioned segmentation templates is set to $1:3:6$. To further enhance diversity, we apply random cropping to both the image and mask. By iterating 10 times over the COCOStuff `train` set, we ultimately generate a training dataset consisting of 1.16M samples.

D ADDITIONAL QUANTITATIVE RESULTS

D.1 MORE RESULTS ON MASK REFINER

We present additional ablation study results on the mask refiner in Tab. 11, evaluated on the `val` split of the refCOCO(+/g) datasets. The findings indicate that both SAM with ViT-L and ViT-H architectures achieve similarly strong performance across all datasets, demonstrating the robustness of the mask refinement process regardless of the test datasets.

Table 11: Ablation study on mask refiner on refCOCO (+/g) datasets.

Method	Refiner	refCOCO val			refCOCO+ val			refCOCOg val		
		cIoU	Acc@0.5	Time (s)	cIoU	Acc@0.5	Time (s)	cIoU	Acc@0.5	Time (s)
Text4Seg	None	73.5	89.3	5.34	67.6	83.6	5.26	69.8	84.0	6.18
Text4Seg	SAM-B	75.5	89.9	5.54	69.8	84.7	5.46	71.3	84.6	6.30
Text4Seg	SAM-L	79.1	90.6	5.73	72.8	85.1	5.63	74.2	85.2	6.58
Text4Seg	SAM-H	79.3	90.0	5.92	72.6	84.3	5.84	74.6	85.6	6.75

Question:

- "Please segment only the [class_name] in the image.",
- "Can you segment the [class_name] in the image?",
- "Where is the [class_name] in this picture? Please respond with segmentation mask.",
- "Where is '[class_name]' in this image? Please output segmentation mask.",
- "Could you provide the segmentation mask for '[class_name]' in this image?",
- "Please segment the image and highlight '[class_name]'."

Answer:

- "Sure, here is the segmentation mask for '[class_name]':",
- "Here is the segmentation map focusing on the [class_name]:",
- "Here is the segmentation mask highlighting the [class_name]:",
- "The segmentation map for '[class_name]' is:",
- "The segmentation mask for '[class_name]' is shown below:",
- "Sure, Here's the segmentation of the [class_name]:",
- "Sure, the segmented output for '[class_name]' is:",
- "Certainly, the segmentation map for '[class_name]' is:",
- "Certainly, here is the segmentation mask for '[class_name]':",
- "The segmentation mask for '[class_name]' is shown below:"

Figure 11: Question-Answer-Template for **partial segmentation** tasks, such as referring segmentation and open vocabulary segmentation tasks. `[class_name]` will be replace with the referring expression in RES datasets or the selected class list in semantic segmentation datasets. The semantic descriptors are appended at the end of each answer.

D.2 More Results on Different Resolution of Semantic Descriptors

Figure 14 provides the complete results across all RES datasets, including refCOCO+. The results indicate that using a 16×16 length of semantic descriptors, combined with the SAM refiner, is an effective approach that delivers strong performance. While it is possible to eliminate the SAM refiner by further increasing the density of semantic descriptors, this would demand significantly higher computational resources, and we will leave this optimization for future work.

D.3 More Results regarding the Mask Refiner

We provide additional quantitative results on Tabs. 12 to 14. While Text4Seg without a mask refiner slightly lags behind LISA and GSVA in terms of average cIoU on referring expression segmentation (RES) tasks, traditional mask refinement techniques, such as Conditional Random Fields (CRF), can be employed to enhance segmentation accuracy. For instance, Text4Seg$_{\text{,InternVL2-8B}}$ with a CRF refiner improves the baseline performance from an average cIoU of 67.5 to 70.1 on RES tasks. Additionally, when using 32×32 semantic descriptors, Text4Seg outperforms its counterpart with 16×16 descriptors. Specifically, Text4Seg$_{\text{,InternVL2-8B}}$ with 32×32 semantic descriptors achieves an average cIoU of 71.4, surpassing LISA's 69.9 and matching GSVA's 71.4 on RES tasks. On the GRES tasks, as shown in the Tab. 13, both CRF and SAM refiners significantly enhance performance, outperforming LISA and GSVA. Notably, Text4Seg$_{\text{,InternVL2-8B}}$ with 32×32 semantic descriptors, even without a mask refiner, achieves performance superior to existing methods. Finally, on the REC tasks, Text4Seg without a SAM refiner continues to outperform current methods, further demonstrating the effectiveness of Text4Seg's visual grounding capabilities.

E Additional Qualitative Results

In this section, we provide more visual examples for different tasks to show the strong capabilities of the proposed Text4Seg.

Question:

- "Please segment the image based on the category: [class_name].",
- "Segment the image according to the specified category: [class_name].",
- "Segment the image while focusing on the category: [class_name].",
- "Please provide a segmentation map for the category: [class_name].",
- "Segment the image with emphasis on the class: [class_name].",
- "Please segment the image, focusing on the candidate category: [class_name].",
- "Could you segment the image, considering the indicated class: [class_name]?"

Answer:

- "Sure, here is the segmentation based on the category '[class_name]':",
- "The image has been segmented according to the category '[class_name]':",
- "Certainly, here is the segmentation map for the category '[class_name]':",
- "The image is segmented with emphasis on the class '[class_name]':",
- "Here is the segmented image focusing on the candidate category '[class_name]':",
- "The image has been segmented with the category '[class_name]' in mind:",
- "Sure, the segmentation mask is:",
- "Sure, the segmented image is:",
- "Certainly, the segmented map is:",
- "Certainly, here is the segmentation mask:",
- "Certainly, here is the segmented output:",
- "Sure, here is the segmentation map:",
- "The segmentation mask is shown below:"

Figure 12: Question-Answer-Template for **conditioned segmentation** tasks like open vocabulary segmentation task. `[class_name]` will be replace with the condition class list in semantic segmentation datasets. The semantic descriptors are appended at the end of each answer.

Referring expression segmentation. Figure 15 provides additional examples of Text4Seg applied to the referring expression segmentation (RES) task. It is evident that Text4Seg can segment objects based on various criteria, including different classes (*e.g.*, “clear glass”), colors (*e.g.*, “blue”), and positions (*e.g.*, “food in the back right”). This versatility demonstrates its superiority in accurately identifying and segmenting objects in complex scenarios.

Referring expression comprehension. We also present additional results on the Referring Expression Comprehension (REC) task in Fig. 16. It is evident that the coarse masks generated by Text4Seg can be effectively utilized for object localization tasks using the simple *mask2box* method. This application highlights the accuracy of Text4Seg in referring object localization, demonstrating its capability to precisely identify and locate objects within complex images.

Open vocabulary semantic segmentation. Figure 17 presents additional examples of Text4Seg performing open-vocabulary segmentation. Notably, Text4Seg demonstrates its ability to segment not only common large objects but also small objects effectively, such as the person and boat on the river. This versatility highlights Text4Seg’s proficiency in accurately identifying and segmenting a wide range of object sizes. Figure 18 illustrates the multi-object segmentation capabilities of Text4Seg. It is evident that Text4Seg successfully segments all identified objects within the image, showcasing its strong ability to handle multiple objects in complex scenarios. This performance highlights its robustness and effectiveness in accurately distinguishing various elements within a single scene.

Visual understanding. Figure 19 presents an example where Text4Seg is used for image captioning, single-object segmentation, and multi-object segmentation. Additionally, Fig. 20 compares the image reasoning capabilities of Text4Seg with the original LLaVA-1.5. While maintaining similar reasoning abilities, our proposed Text4Seg extends functionality by enabling segmentation tasks.

Question:

- "Segment the entire image and classify each category separately."
- "Please perform segmentation on this image and highlight all identifiable elements."
- "Perform segmentation on this image and label all detected categories."
- "Please identify and segment all categories present in the image."
- "Segment the image and label all categories detected."
- "Could you segment the image and label each identifiable category?"
- "Segment the image to identify and label all visible categories."
- "Segment and classify all elements in the image."
- "Identify and segment all categories visible in the image."
- "Can you segment and label the image?"
- "Might you segment this image?"
- "Can you perform segmentation on this image?"
- "Could you please segment this image?"

Answer:

- "Sure, here is the segmented image with each category classified separately:"
- "Sure, here's the segmented image showing all visible categories:"
- "The image is segmented and annotated with each category:"
- "The image segmentation is complete, with all categories marked:"
- "Sure, the segmentation mask is:"
- "Sure, the segmented image is:"
- "Certainly, the segmented map is:"
- "Certainly, here is the segmentation mask:"
- "Certainly, here is the segmented output:"
- "Sure, here is the segmentation map:"
- "The segmentation mask is shown below:"

Figure 13: Question-Answer-Template for **open vocabulary segmentation** tasks. Following LaSagnA (Wei et al., 2024), the class label lists of the test benchmarks are given in the question for fair quantitative comparison. The semantic descriptors are appended at the end of each answer.

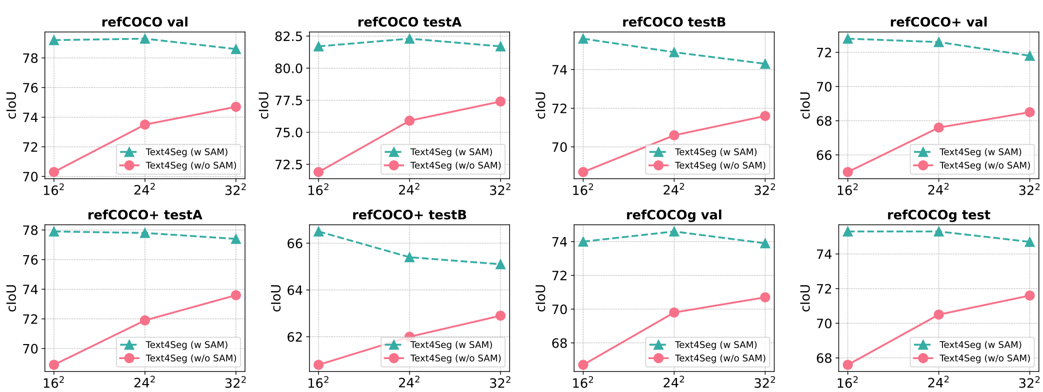

Figure 14: Text4Seg with different resolutions of semantic descriptors on all RES datasets.

Table 12: **Additional Referring Expression Segmentation** results (cIoU) on refCOCO (+/g) datasets. † denotes model is based on the semantic descriptors with a resolution of 32×32.

Methods	Refiner	refCOCO			refCOCO+			refCOCOg		Avg.
		val	testA	testB	val	testA	testB	val	test	
Generalist Segmentation Models ($\leq 8B$)										
LISA (Lai et al., 2024)	-	74.9	79.1	72.3	65.1	70.8	58.1	67.9	70.6	69.9
GSVA (Xia et al., 2024)	-	77.2	78.9	73.5	65.9	69.6	59.8	72.7	73.3	71.4
Text4Seg $_{\text{DeepseekVL-1.3B}}$	None	66.2	68.7	63.6	60.7	64.5	54.9	64.2	64.2	63.4
Text4Seg $_{\text{DeepseekVL-1.3B}}$	SAM-H	75.0	78.6	70.1	68.4	73.4	60.0	71.5	71.7	71.1
Text4Seg $_{\text{DeepseekVL-7B}}$	None	69.7	71.2	67.9	64.5	68.0	60.2	66.6	66.7	66.9
Text4Seg $_{\text{DeepseekVL-7B}}$	SAM-H	78.8	81.5	74.9	72.5	77.4	65.9	74.3	74.4	75.0
Text4Seg $_{\text{LLaVA-1.5-7B}}$	None	70.5	72.3	69.3	64.4	68.7	60.6	65.1	66.5	67.2
Text4Seg $_{\text{LLaVA-1.5-7B}}$	SAM-H	**79.3**	**81.9**	**76.2**	72.1	77.6	66.1	72.1	73.9	74.9
Text4Seg $_{\text{Qwen-VL-7B}}$	None	68.3	70.0	67.3	63.1	67.2	59.9	66.5	77.4	67.5
Text4Seg $_{\text{Qwen-VL-7B}}$	SAM-H	78.0	80.9	74.6	71.6	77.3	66.0	**74.8**	74.7	74.7
Text4Seg $_{\text{InternVL2-8B}}$	None	70.3	71.9	68.7	65.0	68.9	60.8	66.7	67.6	67.5
Text4Seg $_{\text{InternVL2-8B}}$	CRF	73.0	75.2	70.7	67.6	72.1	62.6	68.9	70.3	70.1
Text4Seg $_{\text{InternVL2-8B}}$	SAM-H	79.2	81.7	75.6	**72.8**	**77.9**	**66.5**	74.0	**75.3**	**75.4**
Text4Seg $_{\text{InternVL2-8B}}$ †	None	74.7	77.4	71.6	68.5	73.6	62.9	70.7	71.6	71.7
Text4Seg $_{\text{InternVL2-8B}}$ †	SAM-H	78.6	81.7	74.3	71.8	77.4	65.1	73.9	74.7	74.7
Generalist Segmentation Models (13B)										
LISA (Lai et al., 2024)	-	76.0	78.8	72.9	65.0	70.2	58.1	69.5	70.5	70.1
GSVA (Xia et al., 2024)	-	78.2	80.4	74.2	67.4	71.5	60.9	**74.2**	**75.6**	72.8
Text4Seg $_{\text{LLaVA-1.5-13B}}$	None	71.3	72.9	70.3	65.9	70.0	61.8	66.8	67.6	68.3
Text4Seg $_{\text{LLaVA-1.5-13B}}$	SAM-H	**80.2**	**82.7**	**77.3**	**73.7**	**78.6**	**67.6**	74.0	75.1	**76.2**

Table 13: **Additional Generalized Referring Expression Segmentation** results on the grefCOCO dataset. † denotes model is based on the semantic descriptors with a resolution of 32×32.

Methods	Refiner	Validation Set		Test Set A		Test Set B		Avg.
		gIoU	cIoU	gIoU	cIoU	gIoU	cIoU	
Generalist Segmentation Models ($\leq 8B$)								
LISA (Lai et al., 2024)	-	61.6	61.8	66.3	68.5	58.8	60.6	62.9
GSVA (Xia et al., 2024)	-	66.5	63.3	71.1	69.9	62.2	60.5	65.6
Text4Seg $_{\text{DeepseekVL-1.3B}}$	None	64.3	57.2	62.2	61.2	57.1	54.9	59.5
Text4Seg $_{\text{DeepseekVL-1.3B}}$	SAM-H	69.9	63.2	69.7	67.5	62.3	59.8	65.4
Text4Seg $_{\text{DeepseekVL-7B}}$	None	69.0	62.7	66.3	65.9	62.1	61.1	64.5
Text4Seg $_{\text{DeepseekVL-7B}}$	SAM-H	**74.7**	69.0	74.3	73.0	67.4	66.3	70.8
Text4Seg $_{\text{LLaVA-1.5-7B}}$	None	67.9	61.6	66.2	65.9	60.9	59.8	63.7
Text4Seg $_{\text{LLaVA-1.5-7B}}$	SAM-H	73.6	67.9	74.1	72.8	66.1	64.8	69.9
Text4Seg $_{\text{Qwen-VL-7B}}$	None	68.5	61.1	64.6	63.6	61.1	59.6	63.1
Text4Seg $_{\text{Qwen-VL-7B}}$	SAM-H	74.4	68.1	73.1	71.5	66.7	65.3	69.9
Text4Seg $_{\text{InternVL2-8B}}$	None	68.8	63.1	66.9	67.1	62.1	61.6	64.9
Text4Seg $_{\text{InternVL2-8B}}$	CRF	70.0	66.1	69.4	70.9	63.1	64.1	67.3
Text4Seg $_{\text{InternVL2-8B}}$	SAM-H	74.4	**69.1**	**75.1**	**73.8**	**67.3**	**66.6**	**71.1**
Text4Seg $_{\text{InternVL2-8B}}$ †	None	71.8	65.6	71.2	70.0	64.2	62.5	67.6
Text4Seg $_{\text{InternVL2-8B}}$ †	SAM-H	74.9	68.8	75.4	73.6	67.0	65.1	70.8
Generalist Segmentation Models (13B)								
LISA (Lai et al., 2024)	-	63.5	63.0	68.2	69.7	61.8	62.2	64.7
GSVA (Xia et al., 2024)	-	68.0	64.1	71.8	70.5	63.8	61.3	66.6
Text4Seg $_{\text{LLaVA-1.5-13B}}$	None	69.2	63.9	67.4	67.6	62.7	62.0	65.5
Text4Seg $_{\text{LLaVA-1.5-13B}}$	SAM-H	**74.8**	**69.8**	**75.1**	**74.3**	**68.0**	**67.1**	**71.5**

Table 14: **Additional Referring Expression Comprehension** results (Acc@0.5) on RefCOCO (+/g) datasets. † denotes model is based on the semantic descriptors with a resolution of 32×32.

Methods	Refiner	refCOCO			refCOCO+			refCOCOg		Avg.
		val	testA	testB	val	testA	testB	val	test	
Generalist Segmentation Models ($\leq$ 8B)										
LISA (Lai et al., 2024)	-	85.4	88.8	82.6	74.2	79.5	68.4	79.3	80.4	79.8
GSVA (Xia et al., 2024)	-	86.3	89.2	83.8	72.8	78.8	68.0	81.6	81.8	80.3
Text4Seg $_{\text{DeepseekVL-1.3B}}$	None	83.6	87.3	79.1	78.0	83.6	70.3	78.5	78.8	79.9
Text4Seg $_{\text{DeepseekVL-1.3B}}$	SAM-H	86.4	90.3	81.7	80.5	86.3	72.3	82.4	82.7	82.8
Text4Seg $_{\text{DeepseekVL-7B}}$	None	87.2	90.8	83.4	82.1	88.1	76.8	81.1	81.0	83.8
Text4Seg $_{\text{DeepseekVL-7B}}$	SAM-H	89.6	93.3	85.4	84.2	**90.2**	78.5	84.4	84.7	86.3
Text4Seg $_{\text{LLaVA-1.5-7B}}$	None	89.2	92.0	86.4	83.4	88.6	78.0	81.7	82.4	85.2
Text4Seg $_{\text{LLaVA-1.5-7B}}$	SAM-H	**90.8**	**93.7**	**87.6**	84.7	**90.2**	79.0	84.8	85.0	87.0
Text4Seg $_{\text{Qwen-VL-7B}}$	None	87.2	90.1	83.6	82.1	87.4	76.6	81.5	81.3	83.7
Text4Seg $_{\text{Qwen-VL-7B}}$	SAM-H	89.7	93.0	85.8	84.6	90.1	78.6	85.0	85.1	86.5
Text4Seg $_{\text{InternVL2-8B}}$	None	88.3	91.4	85.8	83.5	88.2	77.9	82.4	82.5	85.0
Text4Seg $_{\text{InternVL2-8B}}$	SAM-H	90.3	93.4	87.5	**85.2**	89.9	**79.5**	85.4	85.4	**87.1**
Text4Seg $_{\text{InternVL2-8B}}^{\dagger}$	None	88.9	92.4	84.1	83.1	88.6	77.3	83.6	83.8	85.2
Text4Seg $_{\text{InternVL2-8B}}^{\dagger}$	SAM-H	89.6	92.6	84.9	83.7	88.8	77.6	84.6	84.8	85.8
Generalist Segmentation Models (13B)										
Shikra (Chen et al., 2023a)	Vicuna-13B	87.8	91.1	81.8	82.9	87.8	74.4	82.6	83.2	84.0
LISA (Lai et al., 2024)	-	85.9	89.1	83.2	74.9	81.1	68.9	80.1	81.5	80.6
GSVA (Xia et al., 2024)	-	87.7	90.5	84.6	76.5	81.7	70.4	83.9	84.9	82.5
Text4Seg $_{\text{LLaVA-1.5-13B}}$	None	89.6	92.3	87.0	84.4	89.0	79.1	82.9	82.9	85.9
Text4Seg $_{\text{LLaVA-1.5-13B}}$	SAM-H	**91.2**	**94.3**	**88.0**	**85.7**	**90.8**	**80.1**	**85.6**	**85.5**	**87.7**


clear glass


blue


bike farthest right cut off


food in the back right


bottom right donut


far right surfboard

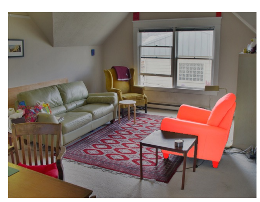
chair on the right

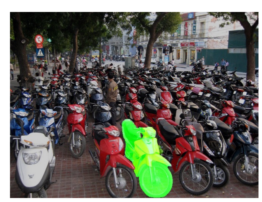
yellow bike


woman washing dishes


pile of green food closest to the end of the bread

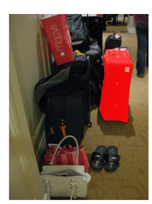
black suitcase on right that is closest to camera


man on upper right near tv

Figure 15: Example results of Text4Seg on referring expression segmentation task. The referring phrases are below the images.

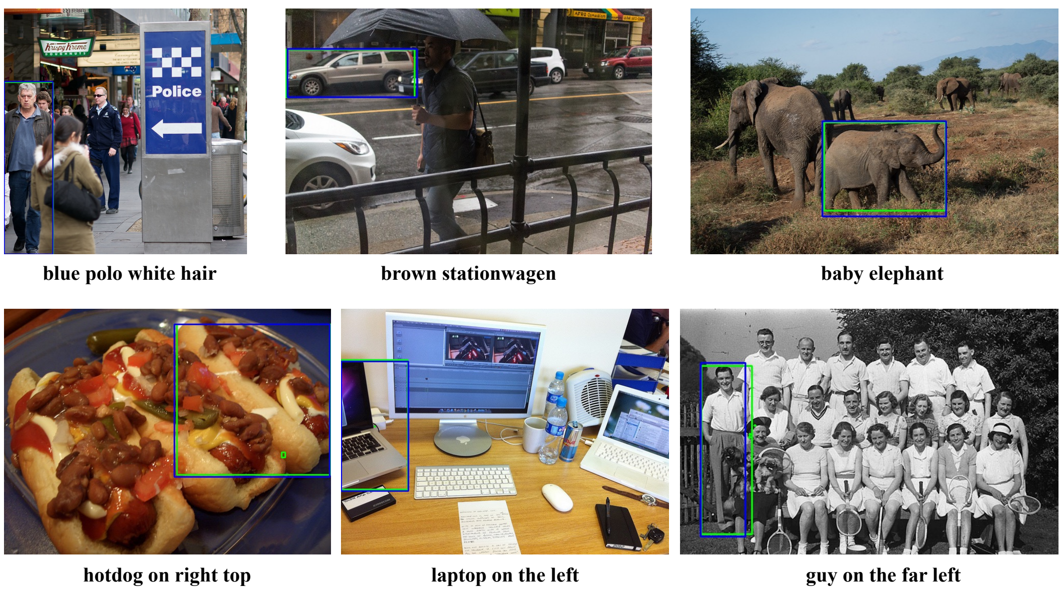

Figure 16: Example results of Text4Seg on referring expression comprehension task. Blue boxes are ground truth labels, and green ones are the Text4Seg predictions.

Query: Can you segment the aeroplane, bicycle, bird, boat, bottle, bus, car, cat, chair, cow, dining table, dog, horse, motorbike, person, potted plant, sheep, sofa, train, TV in the image?

Response: Sure, the segmented mask is:

Figure 17: Example results of open-vocabulary segmentation using Text4Seg on the PAS-20 benchmark.

Query: Can you segment the <PC-59 CLASS LIST> in the image?

Response: Sure, the segmented mask is:

Figure 18: Example results of open-vocabulary segmentation using Text4Seg on the PC-59 benchmark.

Descript this image in detail.

The image depicts a group of wild horses galloping through a grassy field. There are ten horses in total, with some running closer to the foreground and others further back in the scene. The horses are spread out across the field, with some closer to the left side, others in the middle, and a few more towards the right side of the image. The horses appear to be enjoying their time running freely in the open field.

Might you segment the white horse in this image?

Sure, the segmented output for 'white horse' is:

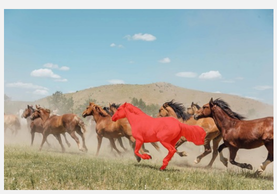

Please segment all horses in the image.

The segmentation mask for 'horses' is shown below:

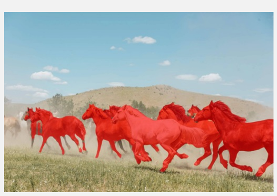

Figure 19: An example result of Text4Seg to perform image captioning, single-object segmentation, and multi-object segmentation.

What is unusual about this image?

Text4Seg

The unusual aspect of this image is that a man is standing on the back of a moving yellow car, holding a clothes dryer. This is not a typical scene, as people usually do not stand on the back of a moving vehicle, especially not on top of a car with a clothes dryer. The man's actions are both dangerous and unconventional, as he could risk falling off the car or causing damage to the vehicle or himself.

LLaVA1.5: The unusual aspect of this image is that a man is standing on a clothesline mounted on the back of a moving yellow car. This is not a common sight, as people typically do not use cars as a platform for hanging clothes or performing other tasks. The man is also wearing a yellow shirt, which adds to the unconventional nature of the scene. The presence of a taxi in the background further emphasizes the unusual nature of the image, as it is not a typical setting for such an activity

Could you please segment this man?

Text4Seg

Sure, here is the segmentation mask for 'man':

LLaVA1.5:

Figure 20: The capability comparison between Text4Seg and LLaVA-1.5.